

# 8. DEVELOPMENT OF DRY POWDER INHALER OF HNCS

## 8.1 INTRODUCTION

In view of the clear advantages of administering a local treatment, delivering chemotherapy directly to the lungs to treat lung tumors has been considered for several decades. As nebulization is the simplest method to deliver a drug to the lungs, inhalation has been achieved by nebulizing liquid drug formulations, i.e., intravenous solution-like formulations, in the first studies, and liposomal dispersions. The state of the art in clinical trials has been reviewed in different works (1). The inhalational route is very convenient for administration compare to other non-oral routes moreover it allows broad distribution window in entire airway. Besides its local action it also accounts for lower systemic adverse effects (2).

The powder based DPI formulations to inhalational route may offer many advantages such as improved stability, low drug loss during administration, improved handling and portability and efficient drug delivery to the pulmonary targeted region (3). Therefore, the development of stable dry powder aerosols for pulmonary gene therapy would be of great benefit. The size of the inhaled formulation particles should not be exceeded than 3  $\mu\text{m}$  (4). Formulation particles which follows this size can reach till the alveoli, are taken up by epithelial cells, and are carried across and released through the systemic blood stream and interstitial fluid compartment between the epithelial cells (4). Other lung formulations of corticosteroids and bronchodilators have size more than 2–3  $\mu\text{m}$  because their targeted region is large bronchi. The particle or droplet size is measured with master sizer equipment or a cascade impactor and is measured with a mass median aerodynamic diameter (MMAD) and its distribution is measured by Geometric standard deviation (GSD) (5).

Lyophilization has acquired as most common method to convert thermolabile and sensitive biomaterials in to a powder form. Effect of lyophilization on siRNA have been studied already by Hattori et al. they have reported that lyophilization of siRNA can be performed in presence of non ionic surfactant as cryoprotectant without tampering with its transfection efficacy (6). In short lyophilization process doesn't

affects its biological activity as well as functionality. The choice of cryoprotectant and cycle of lyophilization affects the stability of the formulation and it should not affect the transfection efficacy of siRNA (7).

The freezing step of lyophilization is operated through cooling of shelves through the glass container in contact. The conduction, convection and radiation are the normal heat transfer modes during lyophilization. The sample has to be cooled from ambient conditions to sub-freezing temperature. During cooling first ice-nucleation occurs several degrees below equilibrium point of sample which is known as “supercooling”. Subsequent to nucleation ice starts to grow and leads to freeze concentration of the sample consisting of two phase i.e. ice and freeze concentrated solution (8-10). The composition of such sample can be obtained by equilibrium freezing-curve of water in the presence of solute. In case of crystalline solutes, the solute crystallization occurs when temperature falls below the eutectic point.

The Cryoprotectant plays an important role in maintaining integrity and preventing freeze fracturing during lyophilization cycle. It also prevents aggregation process during the freezing step of lyophilization if we use it in a proper concentration (11). The particle isolation hypothesis based on separation of unfrozen particles in the unfrozen matrix has been proposed as probable mechanism of stabilization and there is no role of vitrification induced by polymers.

Freeze drying/lyophilization are a composite process of heat transfer and mass transfer simultaneously. During the primary drying process rate of sublimation are controlled either by heat transfer from self and surroundings or by mass of water vapour transfer through the sample. Various methods are used to improve heat and mass transfer process but most successful method is annealing of the frozen sample before the actual process of freeze drying. Annealing process increase the size of the ice crystals and its distribution in the sample which results in the increase heat and mass transfer rate during lyophilization (12, 13). Recently some literature claim that organic solvents are in the formulation increases primary drying rate when compared to formulation containing water (14). Nevertheless, the freeze-drying process generates various stresses during freezing and drying steps. The freezing protocol and

drying conditions have a significant impact on the quality parameters of the final product.

Once lyophilization is completed solid cake needs to be powdered using powderization process which involves shear forces to convert solid cake into free flowing powder (15). Cationic polymers or lipid may reduce the damage caused by shear force to the siRNA by stabilization effect. The powder processing of the lyophilized cakes needs to be performed to convert the poorly flowing mass of solid into a freely flowing, easy to fluidize powder bed which can be dispersed into air stream of respiratory tract in response to the actuation force by the patient during inhalation. Further, literature reports that pDNA condensation induced by cationic agents may minimize damage to pDNA by shear-related forces during powderization (9). Successful gene delivery to the lungs was reported in several studies using polyplex based gene delivery vectors, however a systematic developmental approach involving through in vitro characterization is essential to convert them into practical applications (16).

## 8.2 MATERIALS AND EQUIPEMENTS:

**Table 8-1 List of materials used with their sources**

Sr no.	Name	Supplier of Material
1	Trehalose	Procured from Hi-Media, Mumbai
2	Mannitol	Procured from Hi-Media, Mumbai
3	Respitose SV001	kind gift from DFE Pharma, USA
4	Inhalac 230	Procured from Meggle Pharma, Germany
5.	Acetonitrile	
6.	DEPC treated water	
7.	Double distilled water	

**Table 8-2 List of Equipment Used**

Sr no.	Name of equipment	Company
1.	Virtis Advantage Plus Lyophilizer	Virtis
2.	HPLC	Agilent Technologies 1260 infinity II
3.	Andersen cascade impactor (ACI)	Copley Scientific
4.	SEM instrument- JSM-6380LV	JEOL

### 8.3 PREPARATION AND CHARACTERIZATION OF DPI

#### 8.3.1 Optimization of lyophilization

Cisplatin loaded batches HNCr3 were prepared in nuclease free water then different cryoprotectant such as mannitol and trehalose is added which is filled in Type-1 borosilicate glass prior to lyophilization. All the vials are half Stoppard with grey bromo butyl slotted rubber and kept in the virtis advantage plus, USA lyophilizer. HNCs are subjected to freezing up to  $-40^{\circ}\text{C}$  under the vacuum for continuous 44 hr. Details of the various steps involved in lyophilization such as primary and secondary drying, freezing time ramp and hold temperature are described in the following figure

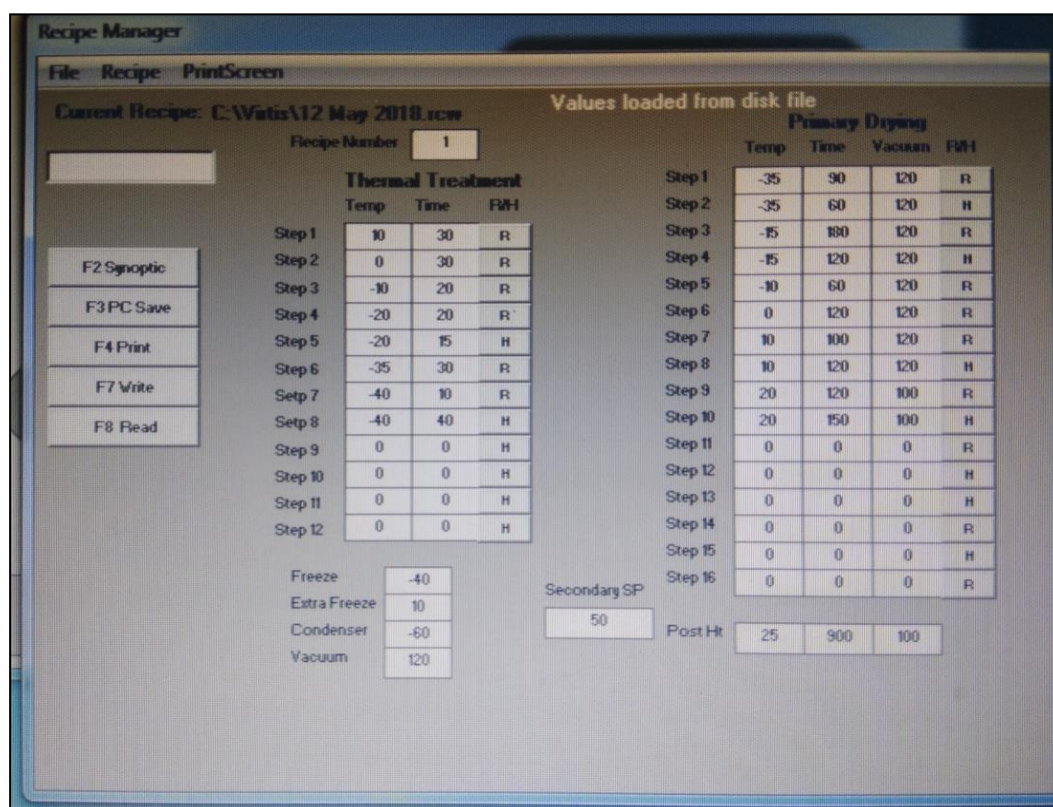


Figure 8-1 Thermal Cycle for Freeze Drying

Beginning of the lyophilization is done with freezing stage. In that shelf temperatures is ramp to  $5^{\circ}\text{C}$  and then hold it for 20 min for the establishment of equilibrium which prevents supercooling effects on the following stages of lyophilization. The freezing stage was begun by ramping the shelf temperature to  $5^{\circ}\text{C}$  and then holding it for 20 min for equilibrium to minimize supercooling effects in subsequent freezing stage. Then temperature was ramped to  $-40^{\circ}\text{C}$  and maintained for

sufficient time to ensure complete freezing. During primary drying the temperatures were maintained below the collapse temperature of the bulking agents. Finally, secondary drying was carried out to remove the bound water and achieve desired moisture content by maintaining the cake at 25°C. The lyophilized vials were kept at 2-8 °C until use. The cryo-protectant out of mannitol and trehalose was selected by studying effect on particle size, zeta potential and integrity of siRNA. The average particle size and zeta potential of siRNA nano-constructs were determined by differential light scattering with a Malvern Zetasizer Nano ZS (Malvern Instruments, Malvern, UK). Prior to the measurement Lyophilized powder were diluted with nuclease free water and measurements were carried out at 25 °C. Zeta potential was calculated by Smoluchowski's equation from the electrophoretic mobility. Each sample was measured three times and the mean values were calculated.

### **8.3.2 Moisture content analysis**

Karl-Fischer titration is widely used method for the determination of moisture in any compound and it is also well established for the lyophilized formulation. Commercially available reagent (pyridine free) was standardized using known amount of water (0.25 kg). For the correction of residual water present in methanol 40 ml of anhydrous methanol was titrated with karl-fisher reagent. After this sample was added and water content was determined by titrimetric procedure.

### **8.3.3 Powder processing and preparation of DPI**

The lyophilized cake was passed through sieve no 120# and 240# which converts the cake in a fine powder. Particle size of the fine powder was evaluated with Differential laser scanning device called Malvern Mastersizer 2000, Malvern UK. The obtained powder was mixed properly with the few inhalational carriers which have characteristic flow properties at a different weight ratio. Ratios from 1/1 to 1/6 were optimised on the basis of improved dispersibility of the DPI during the inhalation. The dry powder formulation was filled in capsule size 3. The lyophilized bulk was processed as described above and filled in hard gelatin capsule size 3 to study aerodynamic behaviour.

### 8.3.4 In-vitro deposition studies

Anderson cascade impactor (ACI) made by Copley scientific was used to determine aerodynamic properties of the dry powder inhaler. Powder for inhalation are filled in size 3 capsules. Capsule is fitted in actuators (ciplahaler) for the dispersion of the powder into cascade impactor. Flow rate was adjusted to the 60 L/min for 4 sec so that volume of 4 L was drawn through the inhaler which creates a pressure drop of 4 kPa. The aim of whole process was to mimic human respiration behaviour. Amount of Cisplatin formulation deposited on each plates and sieves are collected properly with minimal amount of solvent to prevent excessive dilution. The collection of all the sieves and plates are further analyzed by the analytical method.

### 8.3.5 Aerodynamic particle size

ACI has been the traditional choice for classification of particles based on the aerodynamic size. Basic structure of ACI is different stages of different pore size and impaction plate. The DPI was passed through the mouth piece and nozzle and pass through different stages and particles are collected on different plates beneath to each stage. Smaller the particle size it is collected on the lower plates as smaller particles are easily passed from the upper stages. Following figure shows the flow of particle within the Anderson cascade impactor. The flow of the particles of dry powder in the cascade impactor is shown in figure

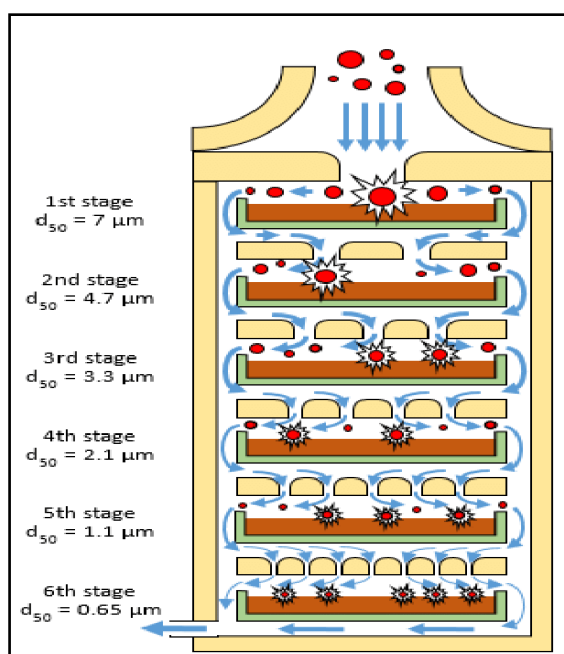


Figure 8-2 Flow of dry powder in the space of cascade impactor.

Every stage with specific cut-off diameter for the particles at a given flow rate affect the separation efficiency of the cascade impactor (17). The sharpness of the collection efficiency curve for given cut-off size in different impactor designed is function of Reynolds number which is generally in the range of 500-3000 to get sharp values.

The respirable fraction which is called as Fine Particle Fraction (FPF), was defined as particle mass below 5  $\mu\text{m}$ . The larger particle fraction or carriers particles would settle in the oropharynx while very small particles are exhaled before undergoing lung deposition. The Aerolizer was primed by connecting with the induction port. Flow meter was installed downstream to impactor and negative pressure was applied to achieve desired flow rate. The ACI was operated at flow rate of 60 L/min and stability was ensured throughout operation. The capsule containing DPI was loaded into the Aerolizer and connected to the induction port and a total of 5 capsules, meeting the requirements of analytical sensitivity, were fired at selected flow rate. At the end the assembly was dismantled and samples were collected by rinsing the walls and collection plate with mobile phase. The fractions collected were analyzed by RP-HPLC to calculate:

1. **Emitted dose (ED):** the amount of dose emitted from the capsule through the inhalation device in to the apparatus.
2. **Fine powder fraction (FPF):** as the fraction of dose found below cut-off diameter  $< 4.7 \mu\text{m}$ .
3. **Recovered dose (RD):** The total amount of dose recovered from the inhalers, capsule shell and the apparatus as % of average assay.
4. **Mass Median Aerodynamic Diameter (MMAD):** The diameter at which 50% mass of particles are larger and 50% smaller. It was determined graphically from the plot of cumulative % mass less than given size on probability scale to log of aerodynamic size. The MMAD is the value of intersect at 50% cumulative percent (18).
5. **Geometric Standard Deviation (GSD):** The GSD was obtained as slope of line or using the formula,

$$\text{GSD} = \frac{\sqrt{d_{84}}}{d_{16}}$$

Where,  $d_{84}$  and  $d_{16}$  are diameters corresponding to 84% and 16% undersize mass, respectively (19).

### 8.3.6 Scanning electron microscopy

In order to get clear insight into the surface characteristics and dry powder characteristics of the prepared dry powder inhaler the particle were subjected to scanning electron microscopy (20). Samples (1-2 mg) were put on double sided adhesive tape attached to the aluminium stub. Then it was exposed to the SEM under 20 KV accelerating voltage. The SEM images were taken by Electrical Research and Development Association (ERDA), Vadodara using SEM instrument-JSM-6380LV, JEOL for the optimized batch of DPI formulation.

### 8.3.7 Powder X-ray diffraction (PXRD)

To study the crystallinity PXRD studies are performed because nature of crystallinity and amorphousness of the dry powder may affect the powder behavior such as adhesive cohesive interactions, flow and fluidization properties, hygroscopicity etc(21). The powder X-ray diffraction pattern was collected from 2-Theta values ranging from 4 to 40.

### 8.3.8 DSC and FTIR

The Lyophilized formulation and cisplatin were studied through Infrared spectrum. This study was carried out to check the compatibility or any significant changes in drug properties during formulation.

### 8.3.9 Integrity of siRNA

The integrity of siRNA after conversion to powder form for inhalation was determined as per procedure described in chapter 6 section 6.3.3 assay procedure.

## 8.4 RESULTS AND DISCUSSION

### 8.4.1 Optimization of lyophilization

The siRNA encapsulated HNCs were formulated as dry powder inhalation product using lyophilization. During the lyophilization water is removed by sublimation in vacuum.

The process consists of freezing the sample and then removing the water by subliming or desorption through vacuum. The stages are categorized into freezing, primary drying and secondary drying. However, first step of freezing the sample into a solid form is most determinant of the integrity of the final product as it impacts the type and size of formed ice crystals, the way of mass transfer during primary and secondary drying (22). It is also said to be the most aggressive step of lyophilization responsible for size growth, aggregation, product concentration etc. Therefore, for successful lyophilization the design of lyo-cycle is important aspect for maintaining product features. There are two types of freezing behaviours. The liquid phase suddenly solidifies at eutectic point, depending on the type of solids in the solution or liquid phase forms a glassy state (does not solidifies), and becomes more and more viscous to form a stiff mass (23).

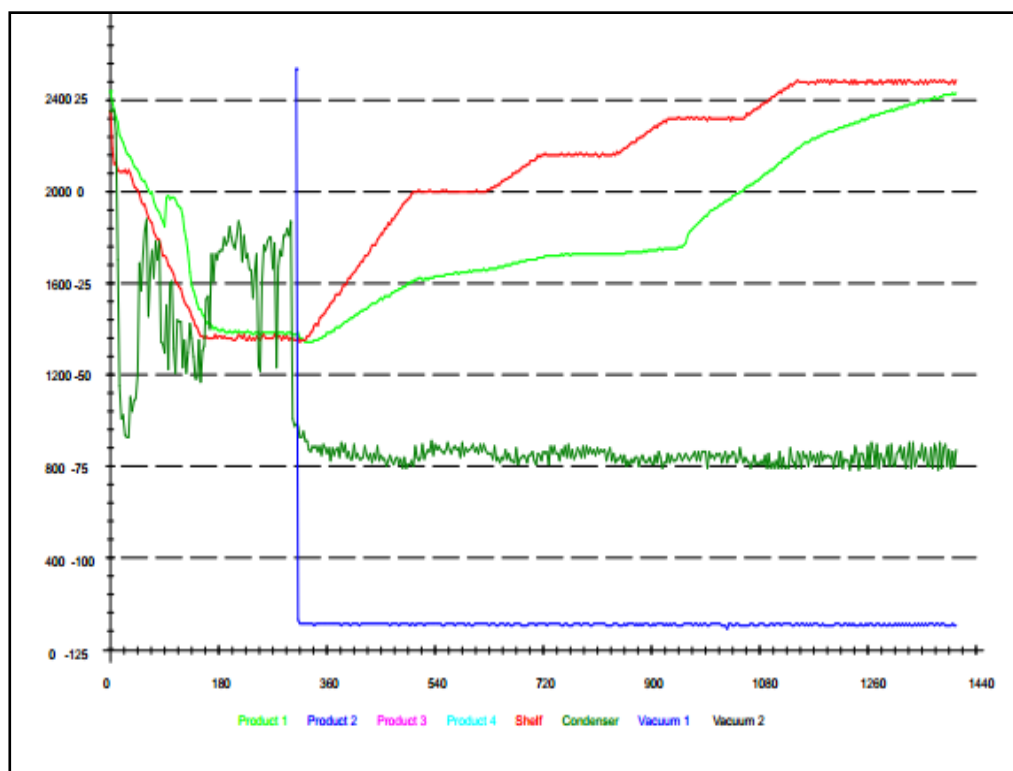


**Figure 8-3 Freeze drying cycle**

The Figure 8-3 shows the effect of freezing rate on super-cooling and nucleation. The larger area of exothermic curve indicates formation of larger ice crystals. Therefore, cooling rate was kept optimum to avoid formation of either very large ice crystals when frozen slowly or formation of very small crystals due to rapid cooling. During freezing, sensible heat is first removed to lower the temperature to the freezing point.

The gradual decrease in temperature with time will continue until reaching the eutectic temperatures for major product components.



**Figure 8-4 lyophilized powder vials**

(A) Lyophilized cake using Lactose (B) Lyophilized cake using Trehalose

Figure 8-4 shows the physical appearance of lyophilized cakes. Although all the cryoprotectants were successfully lyophilized to yield an elegant dry cake, there were differences in physical nature of cake. The cake from Lactose showed shrinkage. The cake formed by trehalose was more homogenous and porous in nature. Therefore, it was expected that trehalose would show better product characteristics.

**Table8-3 Influence of Trehalose in different ratio**

Sr no.	Trehalose Ratio	Before lyophilization			After lyophilization (after reconstitution)		
		Size (nm)	PDI	Zeta potential (mV)	Size (nm)	PDI	Zeta potential (mV)
1	1:2	183.2±0.81	0.182±0.025	25.39±0.183	218.9	0.189	24.48
2	1:4				225.7	0.195	26.71
3	1:6				195.1	0.174	26.79

**Table8-4 Influence of Lactose in different Ratios**

Sr no.	Lactose Ratio	Before lyophilization			After lyophilization (after reconstitution)		
		Size (nm)	PDI	Zeta potential (mV)	Size (nm)	PDI	Zeta potential (mV)

1	1:2	183.2±0.81	0.182±0.025	25.39±0.183	269.9	0.302	21.49
2	1:4				244.7	0.287	29.61
3	1:6				229.2	0.214	28.28

The Table 8.3 and Table 8.4 shows the effect of lyophilization on the physicochemical properties on HNCs R2 placebo batch). The formulations characteristic should be retained after stressful processing of lyophilization. Therefore, after lyophilization the formulations were tested for particle size, PDI, zeta potential, and physical appearance on hydration of cake It was observed that, lyo-cycle selected resulted in aesthetic appearance of cake with good redispersibility in case of trehalose. At the end of the cycle the water content was < 2% w/w in all the cases. The zeta potential values were unaffected after reconstitution.

#### 8.4.2 Moisture content analysis

Table 8-5 Determination of Titer Value

Sr no.	Sample weight in mg	Burette Reading (ml)	Titer Value (mg/ml)	Standard Deviation of Titer value	RSD of Titer value
1	30	4.225	7.100	0.053267	0.753924
2	35	4.997	7.004		
3	38	5.358	7.092		
		Average Titer value	7.0653		

Sr no.	Sample Name	Sample Weight in grams	Burette Reading (ml)	% Water content
1	Trehalose ( 1:2 )	0.1011	0.314	2.19
2	Trehalose ( 1:4 )	0.1023	0.291	2.01
3	Trehalose ( 1:6 )	0.1010	0.270	1.89
1	Lactose ( 1: 2 )	0.1043	0.127	5.2

				HNCs DPI
2	Lactose ( 1: 4 )	0.1023	0.094	5.5
3	Lactose ( 1: 6 )	0.1009	0.084	5.8

**Table 8-6 Determination of moisture content of lyophilized samples**

The DPI with Lactose as cryoprotectant formed clumps in water with poor reconstitubility and therefore could not be extracted enough in the Karl Fisher Reaction medium even on high stirring. Thus the moisture content values appeared low on experimenting. DPI with Trehalose showed low moisture content, favourable characteristics of Size and PDI and thus were selected for further optimization.

#### **8.4.3 Powder processing and preparation of DPI**

Therefore, lyophilized formulation containing trehalose was subjected to powder processing using our previously developed techniques (24-26). The lyophilized cake was size reduced to fines by passing through 120# and 240# (Hitco sieves, Hind Trading Company, Baroda, India). Figure8-5 shows that particle size after sieving. The D50 for the obtained fines was 2.25  $\mu\text{m}$ . Thus obtained fine powder was mixed separately with respitose SV003 and inhalac 230 at different weight ratios, as shown in Table 8.7 and Table 8.8. The blending was performed in geometric mass ratio. The obtained powder mass were then filled in hard gelatin capsules (size 3) and stored in HDPE bottles containing silica bags as desiccant. Meanwhile, the powder prepared was subjected to analysis of powder characteristics for selection of optimum carrier mass ratio.

d(0.1): 1.180 um                      d(0.5): 18.629 um                      d(0.9): 51.975 um

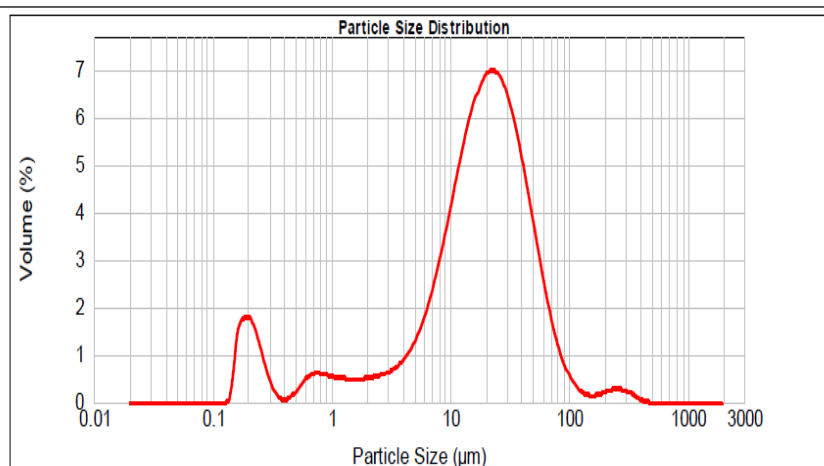


**Figure 8-5 Particle size distribution of DPI**

#### **8.4.4 Aerosolization performance of dry powder for inhalation**

The respirable fraction or fine Particle Fraction (FPF) is defined as particle mass below 5 µm. Aerodynamically light porous particles would lead to enhanced FPF. In current study, the target was set to develop aerodynamically light porous particles having tap density below 0.4 g/cc, mean geometrical diameter above 5 µm and mean MMAD of particles between 1-3 µm to obtain higher FPF and avoidance of natural clearance mechanism in lungs through alveolar macrophage uptake. The larger particle fraction or carriers particles would settle in the oropharynx while very small particles are exhaled before undergoing lung deposition. Thus obtained fine powder was mixed separately with Respitose SV003 and Inhalac 230 at different weight ratios, as shown in Table 5A and Table 5B. The blending was performed in geometric mass ratio. The obtained powder mass were then filled in hard gelatin capsules (size 3) and stored in HDPE bottles containing silica bags as desiccant.

The aerodynamic behaviour data revealed important role of coarse carriers in development of DPI. As shown in Table 5A and Table 5B, in case of both respitose SV003 and inhalac 230 carriers, there was low emitted dose i.e. 52.30% and 51.35% for inhalac 230 and respitose SV003, respectively at lower carrier mass ratios. It was inferred that bulk properties were dominated by lyophilized bulk with sticky/cohesive nature with poor fluidization. The addition of coarse carrier at higher mass ratio led to improvement in emitted dose up to 75.10% and 78.90% for inhalac 230 and respitose SV003, respectively due to improved fluidity. However, the FPF

and MMAD observation revealed differences in inter-particulate forces while using two different carriers. Respirose SV003 showed higher FPF than the Inhalac 230 i.e. 37.48 % and 27.87% respectively at carrier mass ratio of 1:3. Thus, respirose SV003 was selected.

**Table 8-7 Characterization of aerodynamic behaviour using inhalac 230 as carrier**

Sr. No	Carrier mass ratio (w/w)	Recovered Dose (%)	Emitted Dose (%)	MMAD ( $\mu\text{m}$ )	FPF (%)	GSD
1.	1:0	91.0 $\pm$ 1.85	51.35 $\pm$ 3.72	7.16 $\pm$ 0.28	8.51 $\pm$ 0.13	4.5
2.	1:1	93.20 $\pm$ 2.74	66.4 $\pm$ 1.69	6.96 $\pm$ 0.93	11.02 $\pm$ 1.451	3.5
3.	1:3	94.13 $\pm$ 1.94	75.1 $\pm$ 3.27	5.33 $\pm$ 0.57	27.87 $\pm$ 3.17	2.8

**Experiments were performed in triplicate.**

**Table 8-8 Characterization of aerodynamic behaviour using Respirose SV003 as carrier**

Sr. no	Carrier mass ratio (w/w)	Recovered Dose (%)	Emitted Dose (%)	MMAD ( $\mu\text{m}$ )	FPF (%)	GSD
1.	1:0	90.15 $\pm$ 2.59	52.3 $\pm$ 1.68	6.76 $\pm$ 0.45	9.06 $\pm$ 1.19	4.34
2.	1:1	91.09 $\pm$ 1.49	62.4 $\pm$ 2.73	6.30 $\pm$ 0.26	18.41 $\pm$ 4.28	3.70
3.	1:3	93.14 $\pm$ 3.17	78.9 $\pm$ 1.38	3.34 $\pm$ 0.27	37.48 $\pm$ 5.86	2.24

**Experiments were performed in triplicate.**

It was observed that optimized carrier concentration is necessary to achieve detachment of HNCs from carrier molecule leading to higher FPF. This promising aerosolization performance lead to formation of aerodynamic light and large HNCs DPI particles having good flow properties, low density and lesser moisture content. Moreover, particle engineering approach by reducing aerodynamic diameters through porous and low density particles is promising technique to improve aerosolization performance. The theoretical aerodynamic diameter of any inhalational Nanoparticles must lie within range of 1  $\mu\text{m}$  to 5  $\mu\text{m}$  for deep lung deposition. Particles having aerodynamic diameter less than 1  $\mu\text{m}$  are exhaled and particles larger than 5  $\mu\text{m}$  are predominantly deposited in larger airways i.e. mouth and throat. The powder processing leads to enhancement of powder characteristics such as cohesive-adhesive interactions, flow properties, fluidization of the lyophilized bulk (14).

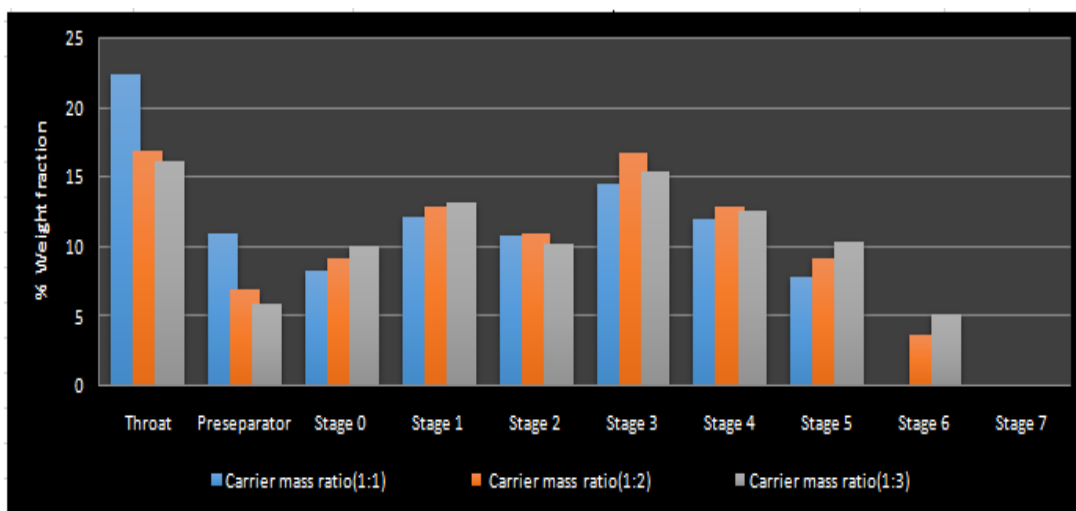


*Figure 8-6 In-vitro pulmonary deposition pattern of dry powder formulations using Respirose SV003*

#### 8.4.5 Scanning electron microscopy

The SEM were performed to study the microscopic features of the dry powder. It can be observed in Figure 8.6 that fines were adsorbed on the surface of carrier particles. The small particles adhere on the energy rich active sites present on the surface of carrier. The carrier particles are easily entrained in the inspiratory air flow from which the adhered particles are then stripped off due to turbulent shear stress and inertial separation mechanisms.

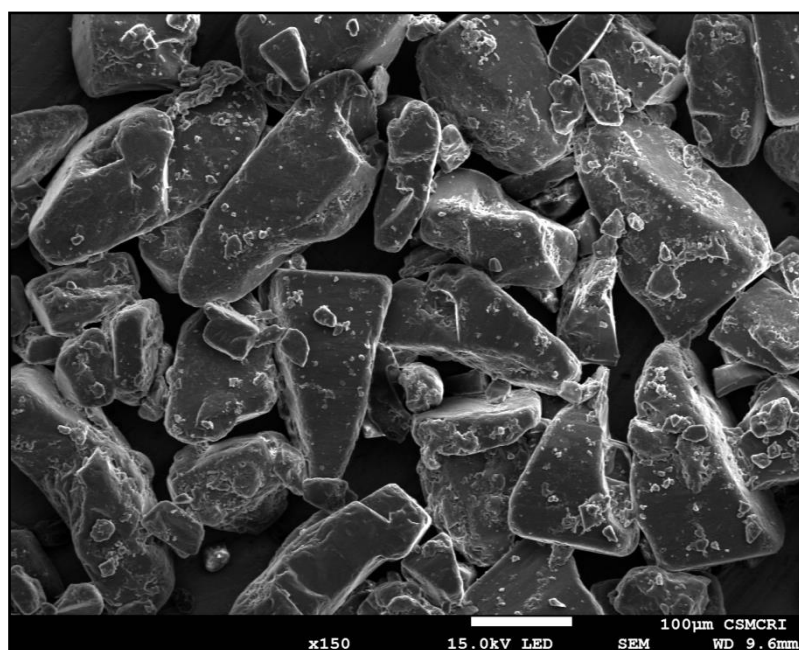


Figure 8-7 SEM image of the optimized blend for DPI formulation HNCs R4

#### 7.4.6 Powder X-ray diffraction (PXRD)

PXRD is emerging as most sensitive and accurate determination methods for a solid-state characterization of dry powder. Results of PXRD are direct reflection of crystallinity of the molecule direct from its atomic structure. From the comparative evaluation of the peak list we can conclude that DPI formulation is more crystalline than pure drug which is required for the smooth flow till the lung alveoli. The higher crystallinity of the DPI could be due to addition of trehalose during lyophilization and powder processing with Respirose SV003 (Figure 8.8). When intensity of 100% relativity compared between Drug and DPI formulation HNCs R4 it shows that DPI formulation has the highest intensity. The 100% peak of the DPI is almost 10 times higher than drug's highest intensity which shows higher crystallinity of the DPI compare to Cisplatin. The presence of crystallinity is suitable for agglomeration and adsorption onto the surface of carrier materials. Amorphous regions have higher surface adhesion energy than crystalline regions which leads to poor de-aggregation after fluidization in air stream. In contrast, crystalline regions interact weakly with and are easily overcome by turbulent shear during inspiration by patient. The crystallinity is also helpful for better flow properties and better chemical stability during shelf storage.

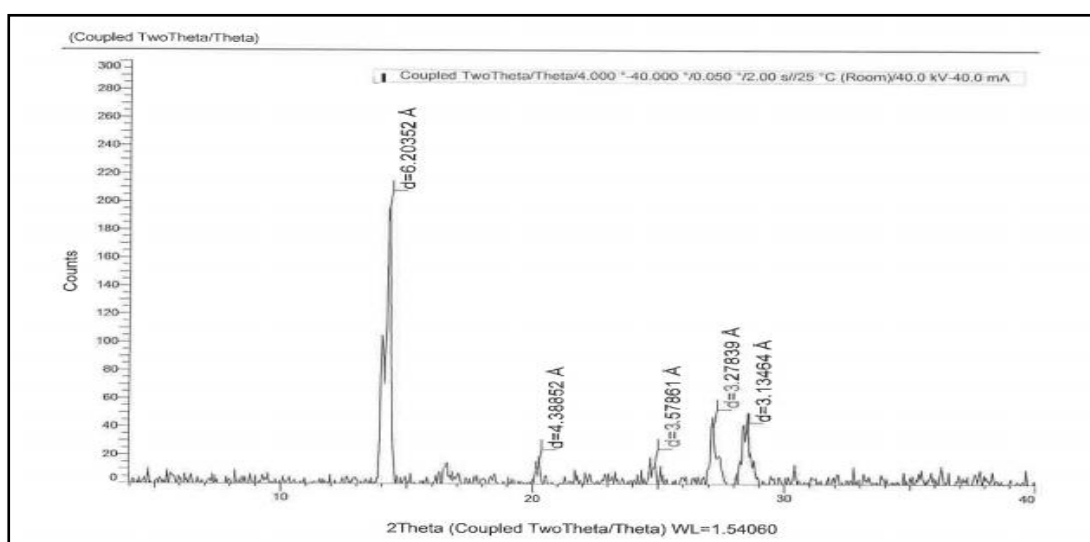


Figure 8-8 PXRD image of Cisplatin

Index	Caption (display)	Angle	d Value	Intensity	Rel. Intensity
1	d=6.20352 Å	14.266 °	6.20352 Å	194.604	100.0 %
2	d=4.38852 Å	20.219 °	4.38852 Å	10.438	5.4 %
3	d=3.57861 Å	24.861 °	3.57861 Å	11.212	5.8 %
4	d=3.27839 Å	27.179 °	3.27839 Å	38.901	20.0 %
5	d=3.13464 Å	28.451 °	3.13464 Å	29.862	15.3 %

Table 8-9 Peak list of the pure drug

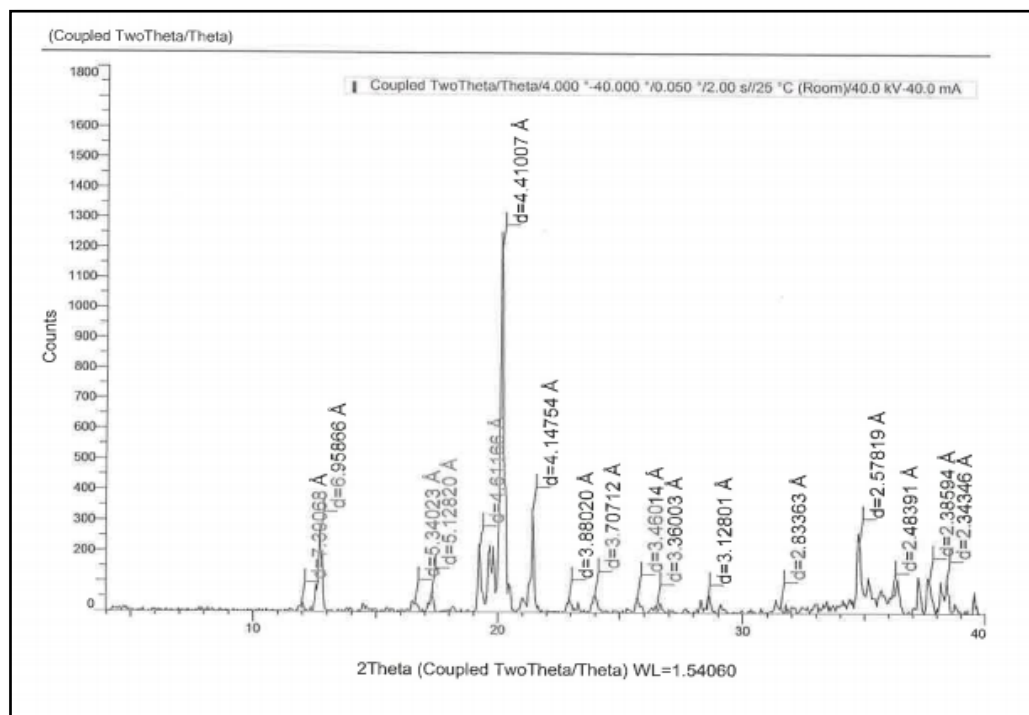


Figure 8-9 PXRD image of developed DPI after powder processing

Table 8-10 Peak list of the DPI

Index	Caption (display)	Angle	d Value	Intensity	Rel. Intensity
1	d=7.39068 Å	11.965 °	7.39068 Å	16.044	1.3 %
2	d=6.95866 Å	12.711 °	6.95866 Å	248.422	20.7 %
3	d=5.34023 Å	16.587 °	5.34023 Å	24.785	2.1 %
4	d=5.12820 Å	17.278 °	5.12820 Å	65.112	5.4 %
5	d=4.61166 Å	19.231 °	4.61166 Å	203.511	17.0 %
6	d=4.41007 Å	20.119 °	4.41007 Å	1197.973	100.0 %
7	d=4.14754 Å	21.407 °	4.14754 Å	330.417	27.6 %
8	d=3.88020 Å	22.901 °	3.88020 Å	27.638	2.3 %
9	d=3.70712 Å	23.986 °	3.70712 Å	56.004	4.7 %
10	d=3.46014 Å	25.726 °	3.46014 Å	44.818	3.7 %
11	d=3.36003 Å	26.506 °	3.36003 Å	12.167	1.0 %
12	d=3.12801 Å	28.513 °	3.12801 Å	12.122	1.0 %
13	d=2.83363 Å	31.548 °	2.83363 Å	22.412	1.9 %
14	d=2.57819 Å	34.768 °	2.57819 Å	231.513	19.3 %
15	d=2.48391 Å	36.132 °	2.48391 Å	52.991	4.4 %
16	d=2.38594 Å	37.671 °	2.38594 Å	102.485	8.6 %
17	d=2.34346 Å	38.380 °	2.34346 Å	92.569	7.7 %

## 8.4.6 FTIR

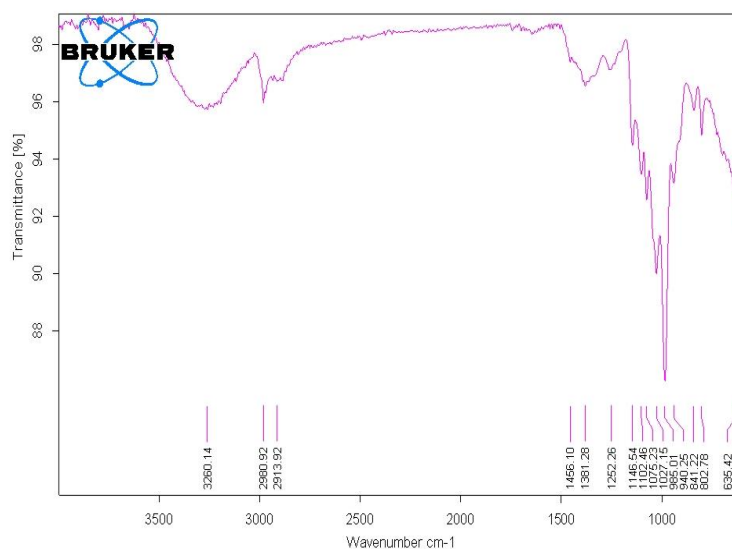


Figure8-10 IR spectra of Cisplatin caprylate loaded DPI

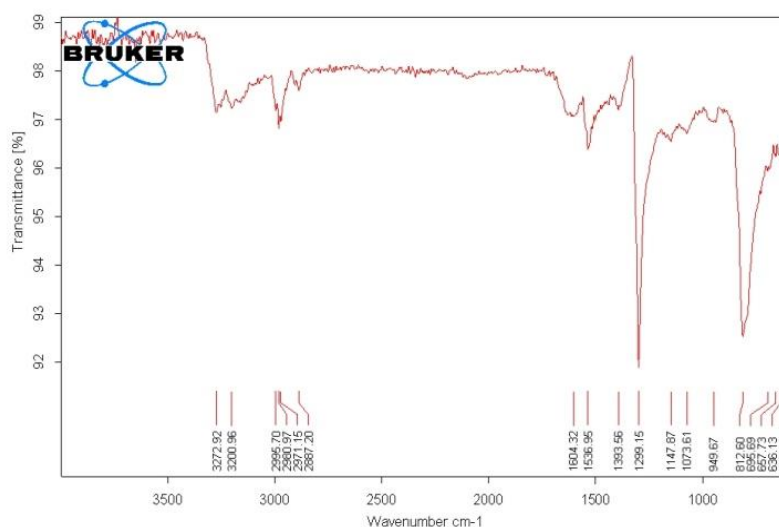


Figure 8-11 IR spectra of Cisplatin caprylate

The characteristic bands were identified in IR spectrum of cisplatin caprylate. IR of DPI formulation was taken to check compatibility of drug and excipients. It exhibited characteristic peaks at 2995 cm<sup>-1</sup> for NH<sub>3</sub> symmetric stretching, 1536 cm<sup>-1</sup> for NH<sub>3</sub> asymmetric deformation, 1299 cm<sup>-1</sup> for NH<sub>3</sub> Symmetric deformation and 948 cm<sup>-1</sup> for Pt-Cl Stretching Vibrations. All these peaks are considered characteristic to Cisplatin caprylate and are prominently observed. Whereas, in case of DPI all characteristic pertaining to Cisplatin caprylate are absent, indicating the enhanced

encapsulation of drug in the HNCs and only a diffused peaks throughout the spectra at wavenumber higher than  $1400\text{ cm}^{-1}$  are observed.

#### 8.4.7 Integrity of siRNA

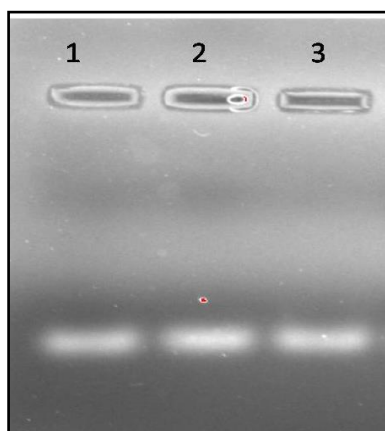


Figure 8-12 integrity of siRNA after DPI formation

*Lane 1: naked siRNA, Lane 2: after lyophilization (HNCs R3), Lane 3: after powder processing (DPI- HNCs-R4)*

From results of band density obtained by gel electrophoresis, it can be concluded that the developed DPI formulations of HNCs retained the integrity of the siRNA even after the lyophilization and powder processing. Table 8-11 shows assay of % complexation of siRNA with HNCs after Lyophilization and powder processing.

Table 8-11 Assay of % complexation of siRNA with HNCs after Lyophilization and powder processing

Formulation	Gel retardation Assay		
	Before lyophilization	After Lyophilization	After powder processing (DPI)
HNCs-R4	97.32 ± 0.192	95.82 ± 0.281	94.21 ± 0.231

## 8.5 REFERENCES

1. Smedsaas-Löfvenberg A, Nilsson K, Moa G, Axelsson I. Nebulization of drugs in a nasal CPAP system. *Acta Paediatrica*. 1999;88(1):89-92.
2. Guillaume C, Delépine P, Droal C, Montier T, Tymen G, Claude F. Aerosolization of cationic lipid–DNA complexes: lipoplex characterization and optimization of aerosol delivery conditions. *Biochemical and biophysical research communications*. 2001;286(3):464-71.
3. Labiris NR, Dolovich MB. Pulmonary drug delivery. Part II: the role of inhalant delivery devices and drug formulations in therapeutic effectiveness of aerosolized medications. *British journal of clinical pharmacology*. 2003;56(6):600-12.
4. Zarogoulidis P, Chatzaki E, Porpodis K, Domvri K, Hohenforst-Schmidt W, Goldberg EP, et al. Inhaled chemotherapy in lung cancer: future concept of nanomedicine. *International journal of nanomedicine*. 2012;7:1551.
5. Levet V, Rosière R, Merlos R, Fusaro L, Berger G, Amighi K, et al. Development of controlled-release cisplatin dry powders for inhalation against lung cancers. *International journal of pharmaceutics*. 2016;515(1-2):209-20.
6. Hattori Y, Hu S, Onishi H. Effects of cationic lipids in cationic liposomes and disaccharides in the freeze-drying of siRNA lipoplexes on gene silencing in cells by reverse transfection. *Journal of liposome research*. 2019 (just-accepted):1-33.
7. Brus C. *Physicochemical and Biological Properties of Polyethylenimine Based Delivery Systems for Oligonucleotides and Ribozymes*; Cuvillier Verlag; 2004.
8. Seville PC, Kellaway I, Birchall J. Preparation of dry powder dispersions for non-viral gene delivery by freeze-drying and spray-drying. *The Journal of Gene Medicine: A cross-disciplinary journal for research on the science of gene transfer and its clinical applications*. 2002;4(4):428-37.
9. Pfeifer C, Hasenpusch G, Uezguen S, Aneja MK, Reinhardt D, Kirch J, et al. Dry powder aerosols of polyethylenimine (PEI)-based gene vectors mediate efficient gene delivery to the lung. *Journal of controlled release*. 2011;154(1):69-76.
10. Kasper JC. *Lyophilization of nucleic acid nanoparticles*; lmu; 2012.
11. Allison SD, dC Molina M, Anchordoquy TJ. Stabilization of lipid/DNA complexes during the freezing step of the lyophilization process: the particle isolation hypothesis. *Biochimica et Biophysica Acta (BBA)-Biomembranes*. 2000;1468(1-2):127-38.
12. Searles JA, Carpenter JF, Randolph TW. Annealing to optimize the primary drying rate, reduce freezing-induced drying rate heterogeneity, and determine Tg' in pharmaceutical lyophilization. *Journal of pharmaceutical sciences*. 2001;90(7):872-87.
13. Rambhatla S, Ramot R, Bhugra C, Pikal MJ. Heat and mass transfer scale-up issues during freeze drying: II. Control and characterization of the degree of supercooling. *Aaps Pharmscitech*. 2004;5(4):54-62.
14. Vessot S, Andrieu J. A review on freeze drying of drugs with tert-butanol (TBA)+ water systems: characteristics, advantages, drawbacks. *Drying Technology*. 2012;30(4):377-85.
15. Shah RB, Tawakkul MA, Khan MA. Comparative evaluation of flow for pharmaceutical powders and granules. *Aaps Pharmscitech*. 2008;9(1):250-8.
16. Brunner S, Sauer T, Carotta Sea, Cotten M, Saltik M, Wagner E. Cell cycle dependence of gene transfer by lipoplex, polyplex and recombinant adenovirus. *Gene therapy*. 2000;7(5):401.

17. Marple VA, Willeke K. Impactor design. *Atmospheric Environment* (1967). 1976;10(10):891-6.
18. Van Holsbeke C, Marshall J, De Backer J, Vos W. Median mass aerodynamic diameter (MMAD) and fine particle fraction (FPF): Influence on lung deposition? *European Respiratory Journal*. 2014;44(Suppl 58):P912.
19. Bakhtiary Z, Barar J, Aghanejad A, Saei AA, Nemati E, Ezzati Nazhad Dolatabadi J, et al. Microparticles containing erlotinib-loaded solid lipid nanoparticles for treatment of non-small cell lung cancer. *Drug development and industrial pharmacy*. 2017;43(8):1244-53.
20. Price R, Young P, Edge S, Staniforth J. The influence of relative humidity on particulate interactions in carrier-based dry powder inhaler formulations. *International journal of pharmaceutics*. 2002;246(1-2):47-59.
21. Kialy W, Nokhodchi A. Freeze-dried mannitol for superior pulmonary drug delivery via dry powder inhaler. *Pharmaceutical research*. 2013;30(2):458-77.
22. Wei W, Mo C, Guohua C. Issues in freeze drying of aqueous solutions. *Chinese Journal of Chemical Engineering*. 2012;20(3):551-9.
23. Mujumdar AS. *Handbook of industrial drying*: CRC press; 2014.
24. Mahesh Kumar T, Misra A. Formulation and evaluation of insulin dry powder for inhalation. *Drug development and industrial pharmacy*. 2006;32(6):677-86.
25. Shah S, Misra A. Development of liposomal amphotericin B dry powder inhaler formulation. *Drug delivery*. 2004;11(4):247-53.
26. Joshi M, Misra A. Dry powder inhalation of liposomal Ketotifen fumarate: formulation and characterization. *International journal of pharmaceutics*. 2001;223(1-2):15-27.